

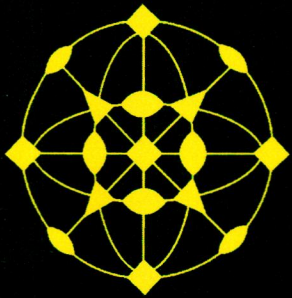
1711  
J80/s2s

Volume 214

June 2014

ISSN 0022-4596

ELSEVIER



# JOURNAL OF SOLID STATE CHEMISTRY

Editor

**M.G. KANATZIDIS**

Associate Editors

**S.J. HWANG**

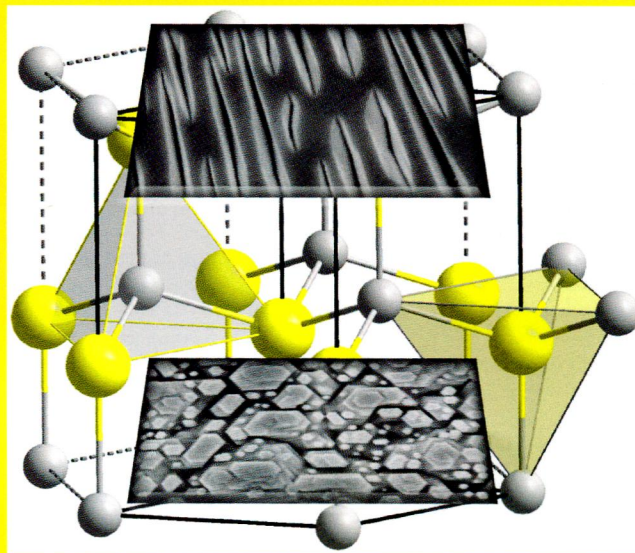
**J. LI**

**S.J. CLARKE**

**H.-C. ZUR LOYE**

## Special Issue

**Innovative processing of inorganic films and nanostructures  
of functional materials, Symposium Q, 7th International  
Conference on Materials for Advanced Technologies,  
30 June to 5 July 2013, Singapore**



**Guest Editor: Dr. Gregory Goh**

Available online at [www.sciencedirect.com](http://www.sciencedirect.com)

**ScienceDirect**

J  
S  
S  
C



Abstracted/indexed in BioEngineering Abstracts, Chemical Abstracts, Coal Abstracts, Current Contents/Physics, Chemical, & Earth Sciences, Engineering Index, Research Alert, SCISEARCH, Science Abstracts, and Science Citation Index. Also covered in the abstract and citation database SCOPUS<sup>®</sup>. Full text available on ScienceDirect<sup>®</sup>.

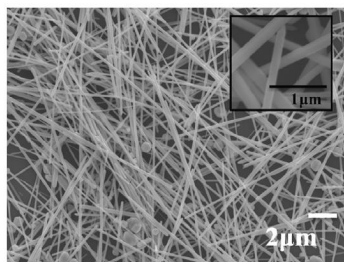
### Editorial

Gregory K.L. Goh  
page 1

### Regular Articles

The concentration effect of capping agent for synthesis of silver nanowire by using the polyol method

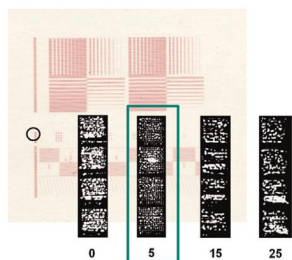
Jian-Yang Lin, Yu-Lee Hsueh and Jung-Jie Huang  
page 2



The FE-SEM image shows that nanostructures with considerable quantities of silver nanowires can also be produced when the PVP (Mw=360 K)/AgNO<sub>3</sub> molar ratio was 2.5.

### Atomic and molecular layer deposition for surface modification

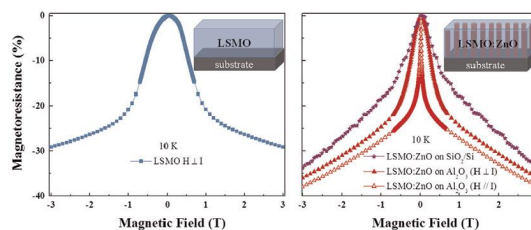
Mika Vähä-Nissi, Jenni Sievänen, Erkki Salo, Pirjo Heikkilä, Eija Kenttä, Leena-Sisko Johansson, Jorma T. Koskinen and Ali Harlin  
page 7



Print quality of a polylactide film surface modified with atomic layer deposition prior to inkjet printing (360 dpi) with an aqueous ink. Number of printed dots illustrated as a function of 0, 5, 15 and 25 deposition cycles of trimethylaluminum and water.

### Regular Articles—Continued

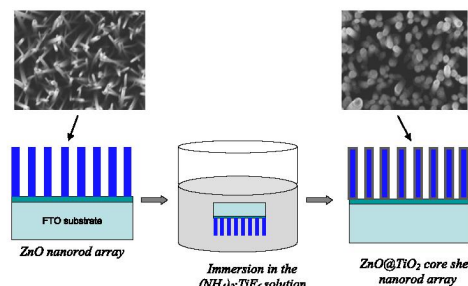
Nanocomposite films with magnetic field sensing properties  
M. Staruch and M. Jain  
page 12



The magnetic field dependent magnetoresistance values at 10 K for La<sub>0.67</sub>Si<sub>0.33</sub>MnO<sub>3</sub> (LSMO) film on Al<sub>2</sub>O<sub>3</sub> substrate are enhanced with addition of secondary phase in LSMO:ZnO nanocomposite films on SiO<sub>2</sub>/Si and Al<sub>2</sub>O<sub>3</sub> substrates. The field sensitivity further increases when the field is applied parallel to the current (H//I).

### Low temperature grown ZnO@TiO<sub>2</sub> core shell nanorod arrays for dye sensitized solar cell application

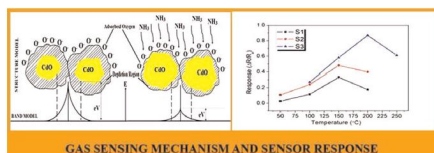
Gregory Kia Liang Goh, Hong Quang Le, Tang Jiao Huang and Benjamin Tan Tiong Hui  
page 17



The synthesis process of coating TiO<sub>2</sub> shell onto ZnO nanorod core is shown schematically. A thin, uniform, and conformal shell had been grown on the surface of the ZnO core after immersing in the (NH<sub>4</sub>)<sub>2</sub>TiF<sub>6</sub> solution for 5–15 min.

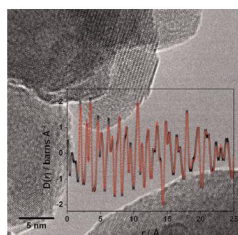
## Magnetron sputtered nanostructured cadmium oxide films for ammonia sensing

P. Dhivya, A.K. Prasad and M. Sridharan  
page 24



## Investigation of some new hydro(solvo)thermal synthesis routes to nanostructured mixed-metal oxides

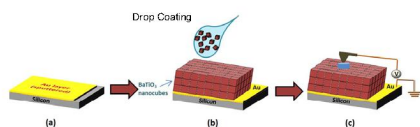
David L. Burnett, Mohammad H. Harunsani, Reza J. Kashtiban, Helen Y. Playford, Jeremy Sloan, Alex C. Hannon and Richard I. Walton  
page 30



New solvothermal synthesis approaches to spinel and rutile mixed-metal oxides are reported.

## Growth and self-assembly of BaTiO<sub>3</sub> nanocubes for resistive switching memory cells

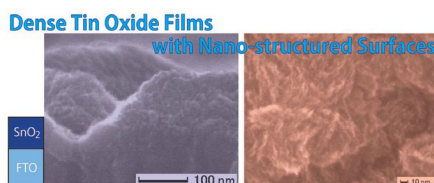
Dewei Chu, Xi Lin, Adnan Younis, Chang Ming Li, Feng Dang and Sean Li  
page 38



This work describes a novel resistive switching memory cell based on self-assembled BaTiO<sub>3</sub> nanocubes.

## Aqueous phase deposition of dense tin oxide films with nano-structured surfaces

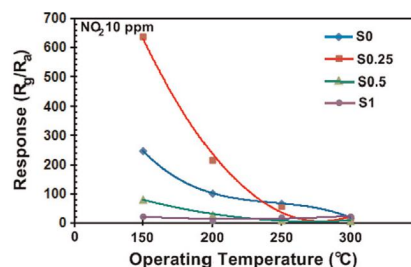
Yoshitake Masuda, Tatsuki Ohji and Kazumi Kato  
page 42



Dense tin oxide films of 65 nm were successfully fabricated in an aqueous solution. They had nano-structured surfaces. Concave-convex substrates were entirely-covered with the continuous films.

## NO<sub>2</sub> gas sensing of flame-made Pt-loaded WO<sub>3</sub> thick films

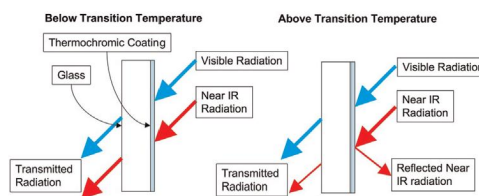
Thanitha Samerjai, Nittaya Tamaekong, Chaikarn Liewhiran, Anurat Wisitsoraat and Sukon Phanichphant  
page 47



The response of 0.25 wt% Pt-loaded WO<sub>3</sub> sensor was 637 towards NO<sub>2</sub> concentration of 10 ppm at 150 °C.

## Chemical vapour deposition of thermochromic vanadium dioxide thin films for energy efficient glazing

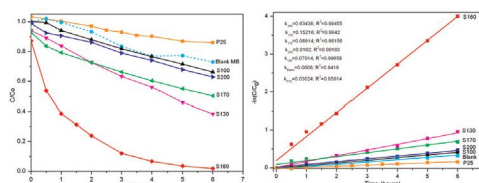
Michael E.A. Warwick and Russell Binions  
page 53



Schematic demonstration of the effect of thermochromic glazing on solar radiation (red arrow represents IR radiation, black arrow represents all other solar radiation).

## One-pot solvothermal synthesis of dual-phase titanate/titania Nanoparticles and their adsorption and photocatalytic Performances

Yu Hua Cheng, Dangguo Gong, Yuxin Tang, Jeffery Weng Chye Ho, Yee Yan Tay, Wei Siew Lau, Olivia Wijaya, Jiexiang Lim and Zhong Chen  
page 67

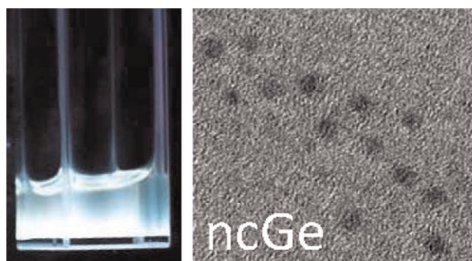


The effect of solvothermal synthesis temperature on the formation and dye removal performance of dual phase titanate/titania nanoparticles was unveiled and optimized.

## Solution-processable white-light-emitting germanium nanocrystals

Naoto Shirahata

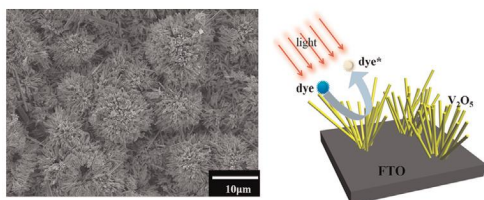
page 74



## Growth of oriented vanadium pentoxide nanostructures on transparent conducting substrates and their applications in photocatalysis

Hongjiang Liu, Yanfeng Gao, Jiadong Zhou, Xinling Liu, Zhang Chen, Chuanxiang Cao, Hongjie Luo and Minoru Kanehira

page 79

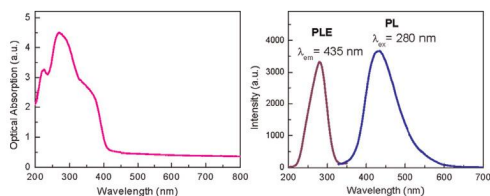


Flower nanostructured vanadium oxide film was prepared by hydrothermal reaction for photocatalysis application.

## Photoluminescence of titanium-doped zinc spinel blue-emitting nanophosphors

Mu-Tsun Tsai, Yec-Shin Chang, You-Hsin Chou and Kai-Min Tsai

page 86

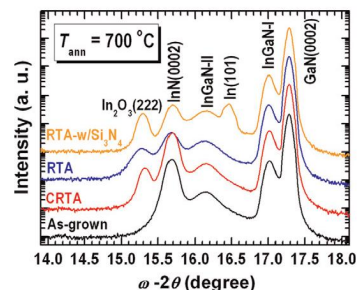


The absorption band around 270 nm is associated with the charge-transfer processes between octahedral  $Ti^{4+}$  and  $O^{2-}$  ions. The excitation band around 280 nm corresponds to the charge-transfer excitations from  $O^{2-}(2p)^6$  electrons to  $Ti^{4+}(3d^0)$ . Under 280 nm excitation, the PL spectrum shows a strong blue emission with a peak at around 435 nm.

## Post-growth thermal oxidation of wurtzite InN thin films into body-center cubic $In_2O_3$ for chemical/gas sensing applications

H.F. Liu, N.L. Yakovlev, D.Z. Chi and W. Liu

page 91

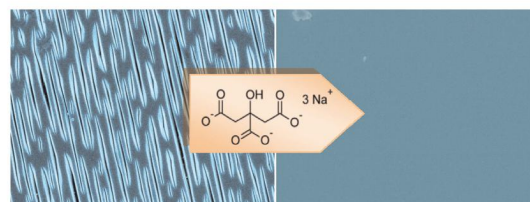


Oxidation of h-InN into bcc- $In_2O_3$  has been realized at elevated temperatures. A  $Si_3N_4$  cap improves the crystal quality of  $In_2O_3$  oxidized by conventional RTA but it results in the presence of undesired metallic indium. Cycle-RTA not only improves the crystal quality but also avoids the byproduct of metallic indium. SIMS depth profiles provide evidence that the oxidation of InN is dominated by oxygen inward diffusion mechanism. The crystal quality of the resultant  $In_2O_3/InN$  heterostructure is mainly controlled by the balance between the speeds of oxygen diffusion and InN thermal dissociation, which can be effectively tuned by cycle-RTA.

## Homoeptaxy of ZnO and MgZnO Films at 90 °C

Dirk Ehrentauf, Gregory K.L. Goh, Katsushi Fujii, Chin Chun Ooi, Le Hong Quang, Tsuguo Fukuda, Masataka Kano, Yuantao Zhang and Takashi Matsuoka

page 96



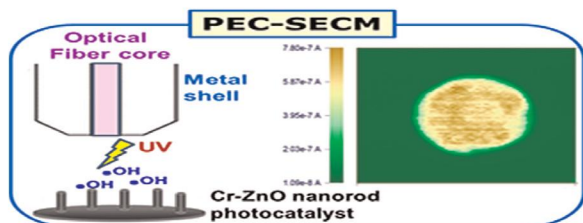
Homoeptaxial ZnO films grown from aqueous solution below boiling point of water on a ZnO substrate with off-orientation reveal parallel grooves that are characterized by  $\{10\bar{1}1\}$  facets. Adding trisodium citrate yields closed, single-crystalline ZnO films, which can further be functionalized. Alloying with MgO yields MgZnO films with low Mg content only.

Continued



## Synthesis and characterization of Cr-doped ZnO nanorod-array photocatalysts with improved activity

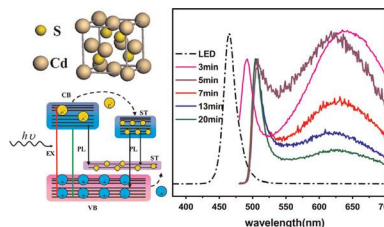
Chi-Jung Chang, Tsung-Lin Yang and Yu-Ching Weng  
*page 101*



Photoinduced charge separation and its relation with the photocatalytic degradation activity of Cr-doped ZnO were investigated by photoelectrochemical scanning electrochemical microscopy.

## White luminescence from CdS nanocrystals under the blue light excitation

Bo Li, Xiaosong Zhang, Lan Li, Mengzhen Li,  
Jianping Xu and Yuan Hong  
*page 108*



Trap-rich CdS nanocrystals were synthesized. Furthermore, white light is produced by mixing broad emission across 500–700 nm from CdS NCs excited by blue light, in combination with the remaining blue light.

**Language services.** Authors who require information about language editing and copyediting services pre- and post-submission please visit <http://www.elsevier.com/locate/languagepolishing> or our customer support site at <http://epsupport.elsevier.com>. Please note Elsevier neither endorses nor takes responsibility for any products, goods or services offered by outside vendors through our services or in any advertising. For more information please refer to our Terms & Conditions <http://www.elsevier.com/termsandconditions>

For a full and complete Guide for Authors, please go to: <http://www.elsevier.com/locate/jssc>

*Journal of Solid State Chemistry* has no page charges.